energies

MDPI

Article

Risk-Averse Stochastic Programming for Planning Hybrid Electrical Energy Systems: A Brazilian Case

Daniel Kitamura [1], Leonardo Willer [1], Bruno Dias [1] and Tiago Soares [2,*]

[1] Electrical Energy Department, Federal University of Juiz de Fora, UFJF, Juiz de Fora 36036-330, Brazil
[2] Center for Power and Energy Systems, Institute for Systems and Computer Engineering, Technology and Science, 4200-465 Porto, Portugal
* Correspondence: tiago.a.soares@inesctec.pt

Abstract: This work presents a risk-averse stochastic programming model for the optimal planning of hybrid electrical energy systems (HEES), considering the regulatory policy applied to distribution systems in Brazil. Uncertainties associated with variables related to photovoltaic (PV) generation, load demand, fuel price for diesel generation and electricity tariff are considered, through the definition of scenarios. The conditional value-at-risk (CVaR) metric is used in the optimization problem to consider the consumer's risk propensity. The model determines the number and type of PV panels, diesel generation, and battery storage capacities, in which the objective is to minimize investment and operating costs over the planning horizon. Case studies involving a large commercial consumer are carried out to evaluate the proposed model. Results showed that under normal conditions only the PV system is viable. The PV/diesel system tends to be viable in adverse hydrological conditions for risk-averse consumers. Under this condition, the PV/battery system is viable for a reduction of 87% in the battery investment cost. An important conclusion is that the risk analysis tool is essential to assist consumers in the decision-making process of investing in HEES.

Keywords: hybrid electrical energy system; stochastic programming; risk analysis; optimization; renewable energy sources

Citation: Kitamura, D.; Willer, L.; Dias, B.; Soares, T. Risk-Averse Stochastic Programming for Planning Hybrid Electrical Energy Systems: A Brazilian Case. *Energies* **2023**, *16*, 1463. https://doi.org/10.3390/en16031463

Academic Editor: Antonio Cano-Ortega

Received: 23 December 2022
Revised: 23 January 2023
Accepted: 27 January 2023
Published: 2 February 2023

1. Introduction

1.1. Motivation and Background

The incentive to renewable energy sources (RES) in Brazil boosted the penetration of distributed energy resources (DER) in distribution systems (DS), highlighting sources of distributed generation (DG), such as PV. From the consumer's perspective, the analysis of investment in DG is based on the comparison between associated costs and electricity tariffs [1]. The Brazilian Regulatory Agency (ANEEL), through Normative Resolution 482/2012 [2], provided conditions to encourage DG in Brazil by establishing a net metering system. In this context, HEESs emerged, which are residential, commercial, or industrial facilities isolated or connected to the main grid, with local generation capacity through diversified sources [3].

The HEES are widely used to supply the demand for electricity in rural communities [4,5] where there is no access to distribution systems. They can also be used to connect to the main grid to enable consumers to reduce their electricity costs. One of the main concerns of the area is the optimal design of these systems, considering aspects such as reliability, and renewable energy, among others.

Among the most important aspects is the relevance of works on HEES planning, which involves the sizing, modeling, and operation of these systems, considering technical and economic aspects. HEES planning is an optimization problem that can contain integer variables, in this case, modeled as mixed-integer programming.

Uncertainties over the decision variables of HEES pose risks to the optimization problem and risk management is important to identify, assess and control possible losses

in economic applications [6]. The financial risk analysis of a consumer in HEES planning problems can consider uncertainties over the RES, load demand, electricity tariff and fuel price.

Therefore, the present work shows a model for the planning of HEES. The model supports the investment and operation of HEES, considering the consumer's risk propensity and uncertainties associated with random parameters.

1.2. Literature Review

Deterministic models have been presented for the planning of HEES [7,8]. The authors in [9] obtain the optimal configuration of a PV/wind/diesel/battery system for a city in the Philippines. The lowest cost was obtained in PV/wind/diesel system. Similarly, the authors in [10] perform the optimal planning of a PV/wind/biomass system, including backup sources such as battery energy storage system (BESS) and diesel generator. The optimal sizing of a grid-connected diesel/PV/fuel-cell system is carried out in [11]. Results showed that the lower use of non-renewable sources to sell/buy energy to/from the grid increases the cost of energy. Similarly, the sizing of a PV/diesel/BESS system for an educational institution is performed in [12]. The analysis is carried out considering the connection or not of the system to the main grid, concluding that the grid-connected system is more economical. The planning of the PV/BESS system for an industrial consumer in Brazil, considering the current net metering system is proposed in [13]. The model determines the better compensation strategy for reducing the cost of energy. Similarly, the authors in [14] perform the planning of a grid-connected PV/diesel/BESS system for residential and commercial consumers, considering the regulatory policies in Brazil. Discussions were made considering four tariff scenarios for commercial and residential consumers. In [15,16] the authors propose the design optimization of a hybrid renewable energy system (HRES) for a university campus. The authors in [17] propose the optimal design of diesel/PV/wind/battery HRES, considering the effects of climate diversity and building energy efficiency on the optimization. In addition, the potential locations to install the system are identified. None of the aforementioned studies considers the intermittent and variable behavior of RES.

To overcome this gap, stochastic models able to handle uncertainties related to random variables of HEES have been proposed [18,19]. The authors in [20] perform the planning of a grid-connected microgrid with demand side management, considering scenarios of load demand and RES. In addition to minimizing cost, the goal is also to maximize customer satisfaction. Results that the model is efficient in determining the microgrid configuration without sacrificing consumer satisfaction. Complementary, Ref. [21] proposes a two-stage stochastic programming model for the optimal sizing of a HEES, in which investment and operation decisions are made in the first and second stages, respectively. The planning was performed for a military base in the U.S. Analysis was made considering key factors such as survivability level, tariff rates, and discount rate. A two-stage model is also introduced in [22] for sizing and operation of HEES, considering uncertainties on load demand and generation, in which clustering methods are applied to define scenarios. The stochastic model is compared with the deterministic one, concluding that the former allows for cost reduction. A two-stage stochastic model for planning HEES is also used in [23,24]. Note that none of these works considers the risk aversion of consumers and operators.

Concerning risk-averse models, reference [25] introduces a risk-averse two-stage stochastic programming for planning HEES, in which the variance is used as a risk metric. Three types of uncertainties were considered: energy demands, solar energy, and wind energy availability. This work does not consider fuel price volatility, i.e., the uncertainty in this variable was not considered The optimal planning of a microgrid with risk analysis that comprises the planning of energy and reserve is addressed in [26] through bi-level stochastic programming model. The upper level determines the capacity of the DG and the respective location in the main grid, while the lower level performs the allocation of switches to define microgrids, using the value-at-risk (VaR) and CVaR metrics. However, this work does not

consider the type of PV panels in the optimization model. In contrast, the authors in [6] propose a model for the optimal operation of HEES, aiming at simultaneously providing energy and reserve, with the CVaR metric being used to measure the decision risk. The reserve is modeled to represent the uncertainties of equipment failure or unpredicted events. The works in [27,28] also consider risk analysis in HEES planning problems. However, the three previous works consider only the operating problem, not contemplating the investment problem.

1.3. Main Contributions

To support the decision-making of investing in HEES, the present work proposes a model for the planning of HEES, considering the regulatory policy applied to DS in Brazil. The objective is to minimize investment and operating costs over the planning horizon. The model provides the number and type of PV panels, diesel generation, and BESS capacity. These technologies are most frequently used for commercial consumers, in which the PV system is used in the net metering system and the diesel generator and battery are used to lower the cost of power at the peak period. A case study involving a real large commercial consumer is introduced.

To do so, this work models uncertainty in the clearness index, load demand, diesel price, and electricity tariff, as well as the risk aversion of consumers in risk-averse stochastic programming. The proposed model evaluates the best configuration of HEES, according to the risk aversion level. Different levels of risk aversion are considered to assess the impact on HEES configuration. The CVaR metric is used.

The novelty of this work is to perform the planning of hybrid systems for the Brazilian regulatory context, considering economic risk analysis and uncertainties in the aforementioned variables.

1.4. Paper Structure

The rest of this paper is organized as follows: Section 2 presents the stochastic model of the uncertain parameters and the CVaR formulation to be applied to the HEES problem. Section 3 presents the proposed HEES planning and operating model. Section 4 assesses the proposed model through a case study involving a real commercial consumer. Section 5 presents the main conclusions.

2. Stochastic and Risk Management Modeling

2.1. Uncertainty Modeling

In the present work, the generation of synthetic scenarios is performed from historical data using probability distribution functions. The uncertainties comprise PV generation, load demand, fuel price for diesel generation, and electricity tariff.

Regarding PV generation, the uncertain variable is solar radiation, represented by the clearness index ($k_{T,t}$). To represent this variable, synthetic data of $k_{T,t}$ is generated, whose stochastic behavior can be statistically modeled by using the distribution of Equation (1), where Γ is the gamma function, a_t and b_t are parameters that are dependent on the expected value and the standard deviation of $k_{T,t}$ [29]. An analogous procedure is performed to generate synthetic data of load demand (l_t), but using the normal distribution of Equation (2), where $E_{ld,t}$ and $\sigma_{ld,t}$ are the corresponding expected value and the standard deviation, respectively.

$$f_{ci,t} = \frac{\Gamma(a_t + b_t)}{\Gamma(a_t)\Gamma(b_t)} k_{T,t}^{a_t - 1}(1 - k_{T,t})^{b_t - 1} \tag{1}$$

$$f_{ld,t} = \frac{1}{\sqrt{2\pi\sigma_{ld,t}^2}} \exp\left[-\frac{(l_t - E_{ld,t})^2}{2\sigma_{ld,t}^2} \right] \tag{2}$$

In relation to the behavior of diesel price and electricity tariff, a process called geometric brownian motion (GBM) is used, as formulated in Equation (3), where B is the value of the variable, n is the period (for instance, a month, quarter or year) and ε is a random component that has a normal distribution with mean value equal to 0 and standard deviation given by the first difference ($DIFF$) of a time series Y [30], according to (4).

$$B_n = B_{n-1} \cdot e^r + \varepsilon \tag{3}$$

$$DIFF_t(Y) = Y_t - Y_{t-1} \tag{4}$$

The synthetic data generated for the random variables are grouped through the k-means algorithm [31], in which an operating scenario s is formed by the aggregated representation of all variables and presents probability π_s. The probability of occurrence of a scenario is given by the division between the number of synthetic data belonging to that scenario and the total number of synthetic data generated. Notice that the value of the variable in a scenario is equal to the average of all the synthetic data belonging to that scenario. The number of scenarios or clusters is defined according to the elbow method, where the minimum number is located in the elbow of the function sum of squared error (SSE) in terms of the number of clusters [32].

2.2. Risk Management

To measure the risks associated with the HEES planning decisions, the CVaR metric is used, which is the expected cost in the $(1-\alpha)$% worst scenarios, where α is the confidence level. Notice that the level of consumer risk propensity is an important factor to assist in decision-making. The CVaR formulation is presented in Equations (5)–(7) [6,33], where ξ and η_s are auxiliary variables, S is the set of scenarios s, and IC and OC_s are the investment and operating costs, respectively.

$$Min\ \text{CVaR} = \xi + \frac{1}{1-\alpha} \cdot \sum_{s \in S} \pi_s \eta_s \tag{5}$$

subject to:

$$(IC + OC_s) - \xi \leq \eta_s\ \forall s \in S \tag{6}$$

$$\eta_s \geq 0\ \forall s \in S \tag{7}$$

3. HEES Planning and Operating Model

The configuration of the HEES considered in this paper is connected to the main grid and includes PV panels, a diesel generator, and BESS. In commercial applications, the PV system is used in the net metering system, the diesel generator to generate power at the peak period (highest tariff), and the battery to arbitrage (charge at the off-peak period and discharge at the peak period). The HEES planning problem in the Brazilian regulatory context is formulated by using a risk-averse stochastic programming model [33] in (8)–(36). In this model, t refers to a time period, s to a scenario, p to the peak load period, op to the off-peak period, and i to a PV panel type. Terms mn and mx as both subscripts and superscripts refer to the minimum and maximum values of the variable at hand, respectively.

$$Min\ \text{OBF} = (1-\beta)\left[TC_{pv} + TC_{dg} + TC_{be} + \sum_{s \in S} \pi_s \left(FC_{dg,s} + EC_{gr,s}\right)\right] + \beta\text{CVaR} \tag{8}$$

subject to:

$$P_{n,pv} \leq D_p \tag{9}$$

$$P_{n,pv} = \sum_{i=1:NI} (P^i_{n,pv} \cdot x_i) \tag{10}$$

$$A^i_{pv} \leq A_{pv,mx},\ \forall i \in \{1, ..., NI\} \tag{11}$$

$$A^i_{pv} = N^i_{pv} \cdot Au^i_{pv},\ \forall i \in \{1, ..., NI\} \tag{12}$$

$$PS_{gr,t,s} + P_{pv,t,s} + P_{dg,t,s} + P_{di,t,s} = PI_{gr,t,s} + P_{ch,t,s} + PL_{t,s},\ \forall t \in T,\ \forall s \in S \tag{13}$$

$$P_{dg,t,s} + P_{di,t,s} + P_{pv,t,s} \leq PL_{t,s} + PS_{gr,t,s} + P_{ch,t,s}\ \forall t \in T,\ \forall s \in S \tag{14}$$

$$P_{pv,t,s} = \eta_{in} \sum_{i=1:NI} (P^i_{pv,t,s} \cdot x_i),\ \forall t \in T,\ \forall s \in S \tag{15}$$

$$\sum_{i=1:NI} x_i = 1 \tag{16}$$

$$0 \leq P_{dg,t,s} \leq P_{dg,n},\ \forall t \in T,\ \forall s \in S \tag{17}$$

$$0 \leq PS_{gr,t,s} \leq M \cdot z_{gr,t,s},\ \forall s \in S \tag{18}$$

$$0 \leq PI_{gr,t,s} \leq M \cdot (1 - z_{gr,t,s}),\ \forall s \in S \tag{19}$$

$$\Delta OP \cdot fa_{opp} + \Delta P \geq 0 \tag{20}$$

$$\Delta OP + \Delta P \cdot fa_{pop} \geq 0 \tag{21}$$

$$\Delta OP = \sum_{t \in OP} (PS_{gr,t,s}) - \sum_{t \in OP} (PI_{gr,t,s}) \tag{22}$$

$$\Delta P = \sum_{t \in P} (PS_{gr,t,s}) - \sum_{t \in P} (PI_{gr,t,s}) \tag{23}$$

$$fa_{opp} = \frac{T_{op,s}}{T_{p,s}} \tag{24}$$

$$fa_{pop} = \frac{T_{p,s}}{T_{op,s}} \tag{25}$$

$$T_{op,s} = \frac{TA_{op,s}}{1 - (\mathrm{ICM} + \mathrm{PIS} + \mathrm{COF})} \tag{26}$$

$$T_{p,s} = \frac{TA_{p,s}}{1 - (\mathrm{ICM} + \mathrm{PIS} + \mathrm{COF})} \tag{27}$$

$$SOC_{t,s} = SOC_{t+1,s} + \left(P_{ch,t,s} \cdot \eta_{be} - \frac{P_{di,t,s}}{\eta_{be}} \right) \cdot \Delta t,\ \forall t \in T,\ \forall s \in S \tag{28}$$

$$\eta_{be} = \sqrt{\eta_{rt}} \tag{29}$$

$$0 \leq P_{ch,t,s} \leq P^{mx}_{ch} \cdot z_{be,t,s},\ \forall t \in T,\ \forall s \in S \tag{30}$$

$$0 \leq P_{di,t,s} \leq P_{di}^{mx} \cdot (1 - z_{be,t,s}),\ \forall t \in T,\ \forall s \in S \tag{31}$$

$$P_{ch}^{mx} \leq \frac{E_{be} \cdot fcd \cdot (SOC_{mx} - SOC_{mn})}{\eta_{ch}} \tag{32}$$

$$P_{di}^{mx} \leq E_{be} \cdot fcd \cdot (SOC_{mx} - SOC_{mn}) \cdot \eta_{di} \tag{33}$$

$$SOC_{mn} \cdot E_{be} \leq SOC_{t,s} \leq SOC_{mx} \cdot E_{be},\ \forall t \in T,\ \forall s \in S \tag{34}$$

$$\left(TC_{pv} + TC_{dg} + TC_{be} + FC_{dg,s} + EC_{gr,s}\right) - \xi \leq \eta_s,\ \forall s \in S \tag{35}$$

$$\eta_s \geq 0,\ \forall s \in S \tag{36}$$

The objective function in (8) consists of minimizing the HEES investment and operating costs that comprise the costs related to the PV system (TC_{pv}), diesel generator (TC_{dg}), storage (TC_{be}), fuel ($FC_{dg,s}$) and energy from the main grid ($EC_{gr,s}$), in addition to CVaR, which is weighted by the risk-aversion level β. The demand cost (TC_d) is fixed and thus directly added to the objective function. Constraint (9) represents the limit of the DG installed capacity, where $P_{n,pv}$ is the PV nominal capacity of (10) and D_p is the contracted demand in the peak period. Constraint (11) limits the PV area (A_{pv}^i) that is calculated in (12), where N_{pv}^i is the number of PV panels and Au_{pv}^i is the area of a PV panel.

The HEES load balancing is given by constraint (13), where $PS_{gr,t,s}$ is the power supplied by the main grid, $PI_{gr,t,s}$ is the power injected to the main grid, $P_{pv,t,s}$ is the PV power, $P_{dg,t,s}$ is the diesel generator power, $P_{di,t,s}$ and $P_{ch,t,s}$ are the discharge and charge power of the battery, respectively, and $PL_{t,s}$ is the load demand. The diesel generator and battery discharge are limited in (14) considering that they provide power only to the load demand. Notice that the diesel generator is not connected to the main grid. The PV power depends on the decision on the panel type as in (15), where $P_{pv,t,s}^i$ is calculated according to [34]. In (16), the discrete variable x_i is used to determine the panel type. The diesel generator power is limited in terms of its nominal value $P_{dg,n}$ through constraint (17). Constraints (18) and (19) avoid the energy from being imported and injected into the main grid at the same time, where M represents a big number. Constraints (20) and (21) prevent excess energy credits occur at the end of the planning horizon. The adjustment factors that adjust the electricity tariff from the off-peak to the peak period and vice-versa, are formulated in (24) and (25), respectively. Constraints (26) and (27) represent the electricity tariff considering the following taxes: (i) tax on circulation of goods and services (ICMS), (ii) the social integration program tax (PIS) and (iii) the tax related to the contributions to financing the social security system (COFINS) [35]. Note that $TA_{op,s}$ and $TA_{p,s}$ are the tariffs excluding these taxes.

The state-of-charge (SOC) of the BESS is formulated in (28) and (29) in terms of the charging (P_{ch}) and discharging (P_{di}) power, and round-trip efficiency (η_{rt}) [14]. Charging and discharging limits are given in (30) and (31), respectively, where $z_{be,t,s}$ is the binary variable ('1' for charging and '0' for discharging) that avoids batteries from charging and discharging at the same time. The SOC limits are in (34), where E_{be} is the BESS capacity (kWh). BESS autonomy, i.e., the maximum period for charging or discharging until the allowable limits is formulated in (32) and (33), where fcd is the charging/discharging factor. The CVaR-related constraints are given in (35) and (36), based on (6) and (7).

The cost of the PV system is given by (37) in terms of the cost of the PV panel type, where $IC_{pv,i}$ is the investment cost [36] and $OC_{pv,i}$ is the annual operation and maintenance (O&M) cost (38) [36]. Factor f_{nv} updates the O&M cost as in (39) and (40), where ny is the planning horizon (years), r_{rd} is the real discount rate, i_{nd} and i_{ir} are the nominal discount and inflation rates, respectively.

The BESS cost is given by (42) and (43), where IC_{be} is the investment cost related to the energy capacity, OC_{be} is the annual O&M cost and $p_{OM,be}$ is a percentage value that varies according to the battery type [37]. In turn, the diesel generator cost is formulated in (44)–(48), where IC_{dg}, OC_{dg}, CC_{dg} and FC_{dg} are the investment, O&M (46) [38], capacity (($/kW)) and fuel costs, respectively [14]. $uc_{dg,t,s}$ and $L_{dg,t,s}$ are the fuel unit cost and consumption, respectively. α_{dg} and β_{dg} depend on the generator type. In (46), f_{dg} is analogous to the factor in (39), but considers the diesel real discount (r_{dg}) and annual updating (i_{dg}) rates.

$$TC_{pv} = \sum_{i=1:NI} ((IC_{pv,i} + OC_{pv,i}) \cdot x_i) \tag{37}$$

$$OC_{pv,i} = 0.005 \cdot IC_{pv,i} \cdot f_{nv} \tag{38}$$

$$f_{nv} = \frac{(1 + r_{rd})^{ny} - 1}{r_{rd} \cdot (1 + r_{rd})^{ny}} \tag{39}$$

$$r_{rd} = \frac{i_{nd} - i_{ir}}{1 + i_{ir}} \tag{40}$$

$$TC_{be} = IC_{be} + OC_{be} \tag{41}$$

$$IC_{be} = CC_{be} \cdot E_{be} \tag{42}$$

$$OC_{be} = p_{OM,be} \cdot IC_{be} \cdot f_{dg} \tag{43}$$

$$TC_{dg} = IC_{dg} + OC_{dg} \tag{44}$$

$$IC_{dg} = CC_{dg} \cdot P_{dg,n} \tag{45}$$

$$OC_{dg} = 0.02 \cdot IC_{dg} \cdot f_{nv} \tag{46}$$

$$FC_{dg,s} = \sum_{t=1}^{NT} uc_{dg,t,s} \cdot L_{dg,t,s} \cdot f_{nv} \tag{47}$$

$$L_{dg,t,s} = \alpha_{dg} \cdot P_{dg,n} + \beta_{dg} \cdot P_{dg,t,s} \tag{48}$$

In the Brazilian regulated contracting environment (ACR), consumers are subject to regulated tariffs and may join the net metering system. The tariffs are subject to corrections called 'flags', according to the generation and cost conditions. The 'green flag' is the base tariff, while the 'yellow' and 'red' represent increases in energy prices. Equation (49) models the energy cost of the main grid ($EC_{gr,s}$), where X is the set of tariff flags x, p_x is the probability of x, f_{en} is analogous to the factor in (39), but considering the energy real discount (r_{en}) and annual updating (i_{en}) rates. Equation (50) model the three possible billing conditions for the exchange between the main grid and the unit consumer [13], where Cf_x is the incremental cost of the flag x. Equation (51) is the probability occurrence of flag X, where $n_{m,x}$ is the number of months with the validity of flag x since the beginning of the tariff flag system and $n_{m,to}$ is the total number of months since the beginning of the tariff flag system. The demand cost is represented in (52), where TD_{op} and TD_p are the demand tariffs, $D_{op,m}$ and $D_{p,m}$ are the contracted demands in the month m and NM is the number of months.

$$EC_{gr,s} = \sum_{x \in X} p_x E_{x,s} \cdot f_{en} \tag{49}$$

$$E_{x,s} = \begin{cases} \sum_{t \in \mathrm{OP}} (PS_{gr,t,s}) \cdot (T_{op,s} + Cf_x) - \\ \sum_{t \in \mathrm{OP}} (PI_{gr,t,s}) \cdot (TA_{op,s} + Cf_x) + \\ \sum_{t \in \mathrm{P}} (PS_{gr,t,s}) \cdot (T_{p,s} + Cf_x) - \\ \sum_{t \in \mathrm{P}} (PI_{gr,t,s}) \cdot (TA_{p,s} + Cf_x), & \text{if } \Delta OP \geq 0 \text{ and } \Delta P \geq 0 \\ \\ \sum_{t \in \mathrm{OP}} (PS_{gr,t,s}) \cdot (T_{op,s} - TA_{op,s}) + \\ \sum_{t \in \mathrm{P}} (PS_{gr,t,s}) \cdot (T_{p,s} + Cf_x) - \\ \left(\sum_{t \in \mathrm{P}} (PI_{gr,t,s}) - \Delta OP \cdot fa_{opp} \right) \cdot (TA_{p,s} + Cf_x), & \text{if } \Delta OP < 0 \text{ and } \Delta P \geq 0 \\ \\ \sum_{t \in \mathrm{OP}} (PS_{gr,t,s}) \cdot (T_{op,s} + Cf_x) - \\ \left(\sum_{t \in \mathrm{OP}} (PI_{gr,t,s}) - \Delta P \cdot fa_{pop} \right) \cdot (TA_{op,s} + Cf_x) + \\ \sum_{t \in \mathrm{P}} (PS_{gr,t,s}) \cdot (T_{p,s} - TA_{p,s}), & \text{if } \Delta OP \geq 0 \text{ and } \Delta P < 0 \end{cases} \tag{50}$$

$$p_x = \frac{n_{m,x}}{n_{m,to}} \tag{51}$$

$$TC_d = \sum_{m=1:NM} \frac{TD_{op} \cdot D_{op,m} + TD_p \cdot D_{p,m}}{1 - (\mathrm{ICM} + \mathrm{PIS} + \mathrm{COF})} \cdot f_{en} \tag{52}$$

4. Case Study

4.1. Case Characterization

In this section, a case study is presented involving a commercial consumer (mall) in a Brazilian city (latitude: 21°41′20″ South, longitude: 43°20′40″ West), whose demand, energy consumption, and roof area were obtained. That is why this region was selected for the study. The mall has an available area for the installation of photovoltaic panels equal to 11,500 m^2. In the present work, 1000 synthetic data were generated for each of the parameters previously mentioned, which were clustered to obtain the scenarios. The number of operating scenarios is defined using the elbow method, which is based on the SSE. Figure 1 presents the curve clusters number x SSE, in which the number of scenarios equal to 10 was chosen, as this value is greater than the elbow points, allowing the representation of a reasonable number of scenarios without an excessive increase in computational effort. The probability occurrence of the ten operating scenarios is shown in Table 1.

The load demand data were represented quarterly, in which each quarter is characterized by a representative day. Representing the data in this way maintains the representativeness of the problem because these data are similar in the same quarter. Figure 2 presents the daily load demand for the consumer in the four quarters of the year in Scenario 1. It can be observed the seasonal influence on the load demand, where the highest load values occur in the summer (first quarter), which is common in Brazil. The load demand data was obtained from a commercial consumer by the authors and has not been published.

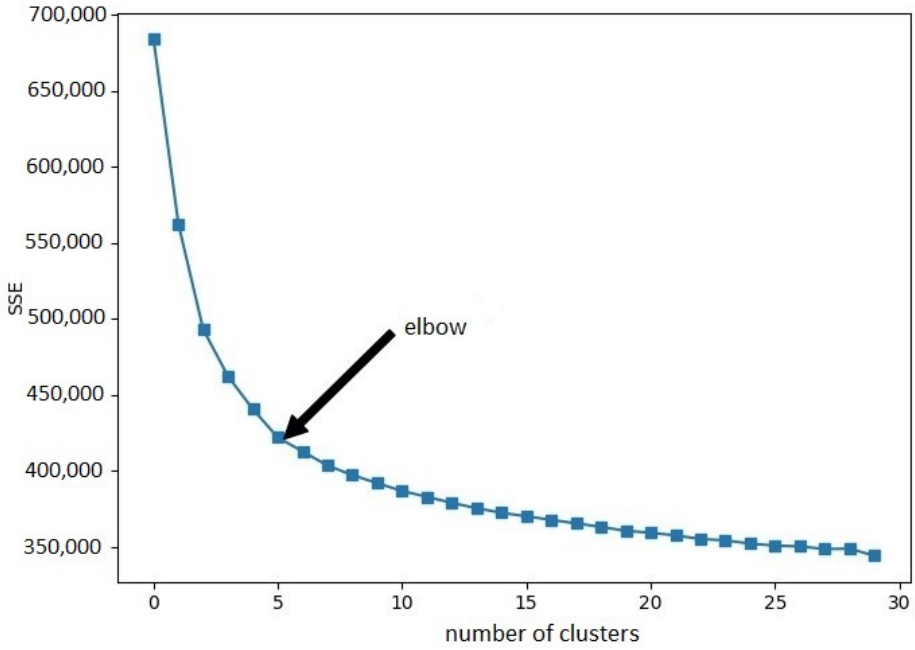

Figure 1. Optimization metric (SSE) in terms of the number of clusters.

Table 1. Probability occurrence of scenarios.

	Scenario 1	Scenario 2	Scenario 3	Scenario 4	Scenario 5
π_s	0.052	0.15	0.123	0.113	0.092
	Scenario 6	Scenario 7	Scenario 8	Scenario 9	Scenario 10
π_s	0.069	0.091	0.116	0.087	0.107

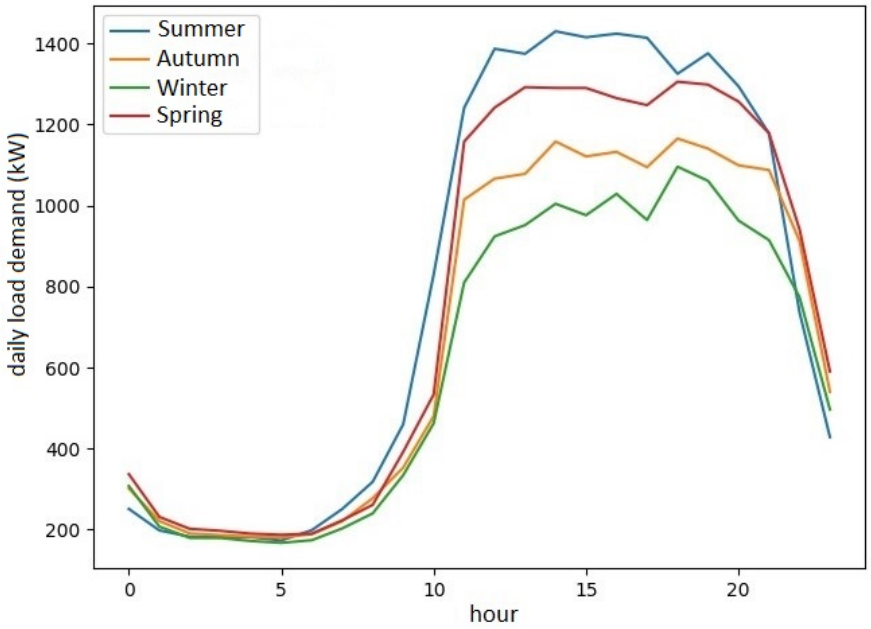

Figure 2. Daily load demand in the four seasons.

The generation of the synthetic clearness index and PV power data for each representative hour/day/quarter was fed by historical global radiation and temperature data from the National Institute of Meteorology (INMET) [39].

The consumer is in the ACR of the Minas Gerais Energy Company (CEMIG), subject to the net metering system and tariffs for energy and power at peak and off-peak periods (blue tariff) [40]. Table 2 presents the tariff structure parameters. Table 3 presents the tariff scenarios for the green flag. The quotation of dollar considered in the present work is R$ 5.50. Four PV panels and one inverter for commercial consumers from the Brazilian market were considered candidates [41]. The specifications of the PV panels and inverter are presented in Tables 4 and 5, respectively. The diesel generator was selected from [38]. In relation to fuel, the diesel S10 price was defined based on historical data from the National Agency for Petroleum, Natural Gas and Biofuels (ANP), and the annual adjustment was calculated based on the mean adjustment since 2013. Table 6 presents the technical specifications of the diesel generator. Figure 3 presents the diesel price scenarios. Notice that the months of the same season have the same diesel price, according to the quarterly discretization.

Table 2. Tariff structure parameters.

D_{op} (kW)	D_p (kW)	$TD_{op,m}$ ($/kW)	$TD_{p,m}$ ($/kW)	PIS (%)	COF (%)
2000	1800	2.70	8.16	5.32	1.15
ICM (%)	i_{tar} [42] (%)	Cf_1 ($/kWh)	Cf_2 ($/kWh)	Cf_3 ($/kWh)	Cf_4 ($/kWh)
25	8.7	0	0.00341	0.00722	0.01726

Table 3. Tariff scenarios for the green flag.

	Scenario 1	Scenario 2	Scenario 3	Scenario 4	Scenario 5
$TA_{op,s}$ ($/kWh)	0.08191	0.06457	0.06923	0.05884	0.06906
$TA_{p,s}$ ($/kWh)	0.11053	0.09319	0.09786	0.08747	0.09768
	Scenario 6	Scenario 7	Scenario 8	Scenario 9	Scenario 10
$TA_{op,s}$ ($/kWh)	0.05026	0.05845	0.07364	0.06525	0.07896
$TA_{p,s}$ ($/kWh)	0.07888	0.08708	0.10226	0.09387	0.10759

Table 4. PV panels specifications.

Type	Manufacturer	Model	Area (m^2)	Cost ($)
1	Canadian Solar	CS3W-420P [43]	2.209184	155.39
2	Canadian Solar	CS3W-395P [44]	2.209184	145.25
3	Risen Solar	RSM156-6-445M [45]	2.060388	185.83
4	Canadian Solar	CS3W-450MS [46]	2.209184	184.14

Table 5. Inverter specifications.

Manufacturer	Model	η_{inv} (%)	CI_{inv} ($/kW)	Lifetime (Years)
ABB	PVS-100/120-TL [47]	98.4	173.69	15

Table 6. Diesel generator specifications.

Manufacturer	Model	α_{dg} (L/kWh)	β_{dg} (L/kWh)	CC_{dg} ($/kW)	i_{dies} (%)
Cummins	C500 D6 [48]	0.015	0.246	100	7.29

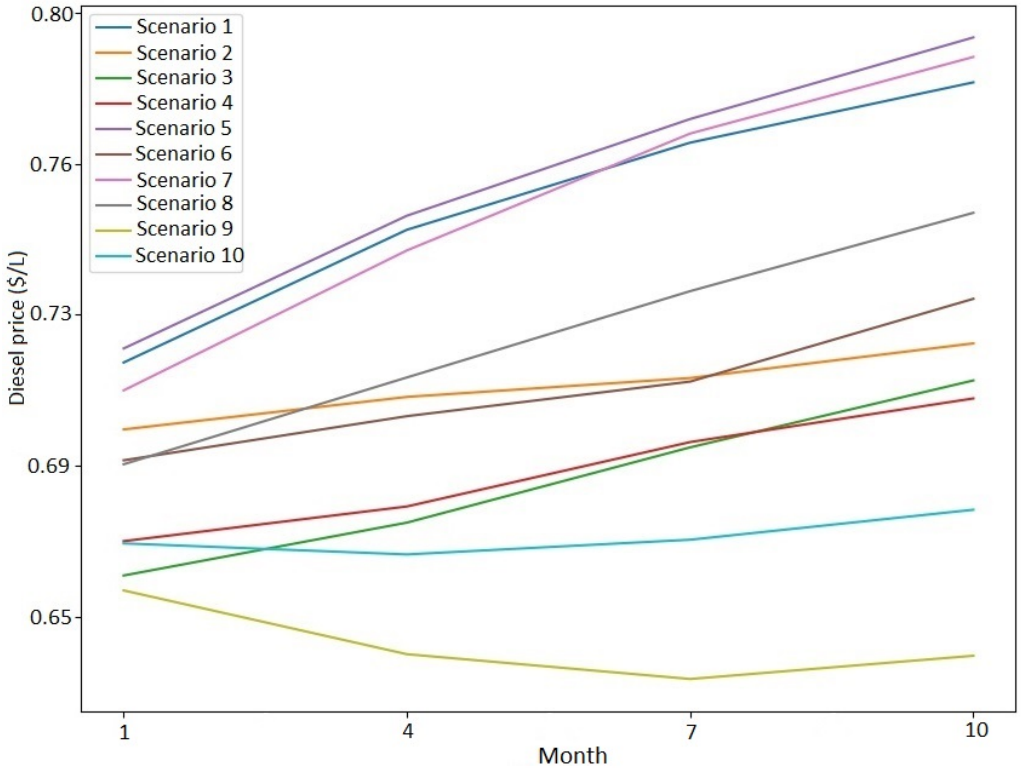

Figure 3. Diesel price scenarios.

The battery is of lithium-ion Nickel-Cobalt-Aluminum (NCA) type. The capacity cost is related to the Brazilian market and is considered that the battery can perform one cycle per day, with a depth of discharge (DOD) of 50%, leading to a maximum number of 9800 cycles. Under these conditions, the battery lifetime is 26 years [37]. The maximum and minimum SOC are 90% and 40%, respectively. The charge/discharge factor (fcd) is 33%, i.e., the battery autonomy is 3 h. This autonomy corresponds to the peak period in Brazil. Table 7 presents the battery specifications [37].

Table 7. Battery specifications—Lithium ion NCA.

Lifecycle [20,50,80] %DOD	Round-Trip Efficiency (%)	$p_{OM,be}$ (%)	CC_{be} ($/kWh)
[77,500,9800,4800]	92	0.25	525.64

4.2. Results

The computer simulations were performed on an AMD Ryzen^{TM} 5 1600 @3.2 GHz, 8 GB RAM, 64-bit operating system, using the Pyomo model and the Gurobi solver. One weekday (with differentiated tariffs according to the period of the day) and one weekend day (without tariff differentiation) were simulated with hourly discretization, totaling 48 h (periods) per quarter for each scenario. The planning horizon is 25 years and the cost is updated to its present value through the factor formulated in (39). The considered inflation rate is the average of the last 25 years, i.e., 6.20%. The nominal discount rate considered is 12%. The demand cost over the planning horizon (TC_d) is equal to \$418,293 $\times 10^3$.

Table 8 presents the results of the proposed model for the most severe 'level-2 red flag' (higher additional cost), considered with occurrence probability at 100% ($p_x = 1$), where 'DG cost' refers to ($TC_{dg} + \sum_{s \in S} \pi_s FC_{dg,s}$), 'EG cost' is equal to ($\sum_{s \in S} \pi_s EC_{gr,s}$). Notice that the model chooses a type-2-PV/diesel hybrid system, except for the lower risk aversion level ($\beta = 0$). In all risk aversion levels, a large PV system was economically feasible in the Brazilian net metering context. Notice that, the net metering policies incentives investment

in this type of technology, which incentives the application of the RES in Brazil. The diesel generator is utilized to generate power in the peak load period, where the electricity tariff is higher. With the increase in the risk aversion level, the diesel generator's capacity increases to be able to supply more power in the peak period in critical scenarios. Moreover, the diesel generator has a higher utilization for $\beta = 1$ (more power) at the peak period to reduce the energy risk at this time. For this condition, the risk aversion level changes the system configuration, which shows that the proposed model assists the decision-making of the consumer.

Table 8. Results for the most severe flag.

	$\beta = 0$	$\beta = 0.2$	$\beta = 0.4$	$\beta = 0.6$	$\beta = 0.8$	$\beta = 1$
N^i_{pv}	4556	4556	4556	4556	4556	4556
P^i_{pv} (kW)	1799.62	1799.62	1799.62	1799.62	1799.62	1799.62
TC_{pv} ($\times 10^3$)	1747.67	1747.67	1747.67	1747.67	1747.67	1747.67
$P_{dg,n}$ (kW)	0	1046.09	1090.52	1101.89	1126.63	1137.73
DG cost ($\times 10^3$)	0	1527.78	1582.34	1594.28	1592.67	1993.52
EG cost ($\times 10^3$)	8680.29	7157.75	7105.36	7093.80	7097.20	7202.96
OBF ($\times 10^3$)	10,427.96	10,604.83	10,775.86	10,945.83	11,115.43	11,284.77
CVaR ($\times 10^3$)	11,776.60	11,291.34	11,286.60	11,285.88	11,284.90	11,284.77

Considering all tariffs with their respective probability shown in Table 9 (normal conditions), Table 10 shows that the proposed model determines a large type-2-PV system at all risk levels β. In this case, the diesel generator is not economically feasible due to the low probability of the most severe 'level-2 red flag' (the diesel generator is economically viable in all risk aversion levels (except for $\beta = 0$) if this flag had a 100% probability of occurrence.). The diesel generator tends to be viable when the most severe flags, i.e., red flags, have a higher probability of occurrence. In other words, these flags are in effect for a longer period, which configures adverse hydrological conditions.

Table 9. Probability occurrence of all tariff flags.

	Green	**Yellow**	**Red Level 1**	**Red Level 2**
p_x	0.3875	0.2	0.2625	0.15

Table 10. Results including all flags.

	$\beta = 0$	$\beta = 0.2$	$\beta = 0.4$	$\beta = 0.6$	$\beta = 0.8$	$\beta = 1$
N^i_{pv}	4556	4556	4556	4556	4556	4556
P^i_{pv} (kW)	1799.62	1799.62	1799.62	1799.62	1799.62	1799.62
TC_{pv} ($\times 10^3$)	1747.67	1747.67	1747.67	1747.67	1747.67	1747.67
EG cost ($\times 10^3$)	7526.14	7526.14	7526.14	7526.14	7526.14	7649.40
OBF ($\times 10^3$)	9273.81	9486.45	9699.10	9911.74	10,124.39	10,318.10
CVaR ($\times 10^3$)	10,633.46	10,337.03	10,337.03	10,337.03	10,337.03	10,318.10

Based on the previous result, an analysis is carried out to investigate the economic viability of the diesel generator, considering the condition mentioned above. That is, based on a gradual increase in the probability of occurrence of the red flag level 2, with a consequent decrease in the probability of the other flags, the scenario for the diesel generator to be economically viable is sought. The simulations were performed for $\beta = 1$, in which it was concluded that for the generator to be economically viable, probabilities shown in Table 11 must occur. Table 12 shows the results for the adverse hydrological conditions.

Table 11. Probability occurrence of all tariff flags—Hydrological adverse conditions.

	Green	**Yellow**	**Red Level 1**	**Red Level 2**
p_x	0.3298	0.1702	0.2234	0.2766

Table 12. Results for the hydrological adverse conditions.

	$\beta = 0$	$\beta = 0.2$	$\beta = 0.4$	$\beta = 0.6$	$\beta = 0.8$	$\beta = 1$
N^i_{pv}	4556	4556	4556	4556	4556	4556
P^i_{pv} (kW)	1799.62	1799.62	1799.62	1799.62	1799.62	1799.62
TC_{pv} ($\$ \times 10^3$)	1747.67	1747.67	1747.67	1747.67	1747.67	1747.67
$P_{n,dg}$ (kW)	0	0	0	0	0	995.59
DG cost ($\$ \times 10^3$)	0	0	0	0	0	1734.48
EG cost ($\$ \times 10^3$)	7698.03	7698.03	7698.03	7698.03	7698.03	6552.07
OBF (R$ $\times 10^3$)	9445.70	9658.08	9870.46	10,082.84	10,295.22	10,506.37
CVaR (R$ $\times 10^3$)	10,803.72	10,507.59	10,507.59	10,507.59	10,507.59	10,506.37

The results presented in Table 12 show that at the other risk aversion levels, the diesel generator is not economically viable, with the system consisting only of PV panels. In adverse hydrological conditions, the tendency is for the diesel generator to be viable for higher risk aversion levels. That is, for a more risk-averse consumer, investing in a diesel generator can be attractive in such scenarios from an economic point of view.

In the previous simulations, the battery was not economically viable due to its high investment cost. Therefore, an additional analysis is carried out to determine the capacity cost of the battery that makes the investment feasible and replaces the diesel generator, considering the adverse hydrological condition (Table 11) and $\beta = 1$. Through exhaustive tests, a viable capacity cost of 67.27 [$/kWh] was identified, that is, there should be a reduction of 87.20% in the cost shown in Table 7. Considering this viable cost for $\beta = 1$, 67.27 [$/kWh], Table 13 presents the costs and the system configuration for different risk aversion levels. Furthermore, Table 13 shows that, with the exception of $\beta = 0$, the CVaR changed little, being equal from $\beta = 0.4$ to $\beta = 1$. In other words, the risk of the operation is practically the same when the battery is inserted into the system. The battery has a large capacity to supply the demand of the consumer. Notice that this technology is applied to arbitrage, that is, the charge is performed at the off-peak period (low tariff) and the discharge at the peak period (highest tariff).

Table 13. Results for the cost that makes the battery viable in adverse hydrological conditions.

	$\beta = 0$	$\beta = 0.2$	$\beta = 0.4$	$\beta = 0.6$	$\beta = 0.8$	$\beta = 1$
N^i_{pv}	4556	4556	4556	4556	4556	4556
P^i_{pv} (kW)	1799.62	1799.62	1799.62	1799.62	1799.62	1799.62
TC_{pv} ($\$ \times 10^3$)	1747.67	1747.67	1747.67	1747.67	1747.67	1747.67
E_{be} (kWh)	6278.71	6242.31	6227.84	6227.84	6227.84	6227.84
TC_{be} ($\$ \times 10^3$)	436.60	434.07	433.07	433.07	433.07	433.07
EG cost ($\$ \times 10^3$)	6996.59	6999.13	7000.15	7000.15	7000.15	7404.61
OBF ($\$ \times 10^3$)	9180.87	9386.16	9591.44	9796.71	10,001.99	10,207.26
CVaR ($\$ \times 10^3$)	10,505.32	10,207.30	10,207.26	10,207.26	10,207.26	10,207.26

5. Conclusions

This work presented a model for planning HEES in the Brazilian regulatory context, through risk-averse stochastic programming, considering uncertainties in the variables clearness index, load demand, diesel price, and electricity tariff, which is the novelty of

this work. The configuration and capacity of the system components were determined to minimize the investment and operating cost in a planning horizon. A Case study involving a large commercial consumer was carried out. From the results, one can be concluded that risk analysis is important to support consumers' decision-making regarding investing in HEES. The configuration and size of the system depend on the current tariff flag, as well as on the consumer's propensity to risk. Under normal conditions, only a large PV system is feasible. Under adverse hydrological conditions, the PV/diesel system is viable for more risk-averse consumers. In the latter condition, the pv/battery system is viable for a reduction of 87.20% in the investment cost of the battery, which indicates the need for incentive policies for this technology to be widely used in the Brazilian market. The main outcome of this work is that studies such as the one proposed in this paper have the potential to subsidize the decision-making process of commercial investors, considering different technological options, trends on random variables through scenarios and appropriate analysis of risks inherent to the process. It is noteworthy that the combination of all these aspects in the decision-making process is an innovative aspect of this work. Given these outcomes, the promising continuation is the inclusion of new economic and environmental variables besides, new regulatory trends, such as those listed in [49], in the referred decision-making process. Therefore, the proposed model has the potential as a tool for planning HEES, aiming at sustainable projects with benefits for consumers. For future work, the authors indicate including reliability analysis on the problem and other sources of distributed generation, such as biomass. In addition, the authors indicate performing simulations on the software HOMER to perform a comparative analysis of the results obtained and therefore evaluate the proposed model.

Author Contributions: Conceptualization, D.K., L.W., B.D. and T.S.; Data curation, D.K. and L.W.; Formal analysis, D.K., L.W., B.D. and T.S.; Investigation, D.K. and L.W.; Methodology, D.K. and L.W.; Supervision, L.W., B.D. and T.S.; Validation, D.K. and L.W.; Writing—original draft, D.K. and L.W.; Writing—review & editing, D.K., L.W., B.D. and T.S. All authors have read and agreed to the published version of the manuscript.

Funding: This research was supported in part by Coordenação de Aperfeiçoamento de Pessoal de Nível Superior (CAPES) under Grant 001, Conselho Nacional de Desenvolvimento Científico e Tecnológico (CNPq) under the grants 404068/2020-0, Fundação de Amparo à Pesquisa do Estado de Minas Gerais (FAPEMIG) under grant APQ-03609-17, and Instituto Nacional de Energia Elétrica (INERGE). It is also supported by Norte Portugal Regional Operational Programme (NORTE 2020), under the PORTUGAL 2020 Partnership Agreement, through the European Regional Development Fund (ERDF), within the DECARBONIZE project under agreement NORTE-01-0145-FEDER-000065 and by the Scientific Employment Stimulus Programme from the Fundação para a Ciência e a Tecnologia (FCT) under the agreement 2021.01353.CEECIND.

Data Availability Statement: Not applicable.

Conflicts of Interest: The authors declare no conflict of interest.

Acronyms

HEES	Hybrid electrical energy systems
PV	Photovoltaic
CVaR	Conditional value at risk
RES	Renewable energy sources
DER	Distributed energy resources
DS	Distribution systems
DG	Distributed generation
ANEEL	Brazilian Regulatory Agency
BEES	Battery energy storage system
VaR	Value-at-risk
SSE	Sum of squared error

GBM	Geometric brownian motion
SOC	State of charge
O&M	Operation and maintenance
ACR	Brazilian regulated contracting environment
INMET	National Institute of Meteorology
CEMIG	Minas Gerais Energy Company
ANP	National Agency for Petroleum, Natural Gas and Biofuels
NCA	Nickel-Cobalt-Aluminum
DOD	Depth of discharge

References

1. Castro, N.; Dantas, G. Distributed Generation: International Experiences and Comparative Analyses; In *Grupo de Estudos do Setor Elétrico*; Publit: Rio de Janeiro, Brazil, 2017; pp. 1–224
2. ANEEL. Resolução Normativa 482. 2012. Available online: http://www2.aneel.gov.br/cedoc/bren2012482.pdf (accessed on 23 September 2021).
3. Fodhil, F.; Hamidat, A.; Nadjemi, O. Potential, optimization and sensitivity analysis of photovoltaic-diesel-battery hybrid energy system for rural electrification in Algeria. *Energy* **2019**, *169*, 613–624. [CrossRef]
4. Islam, M.R.; Akter, H.; Howlader, H.O.R.; Senjyu, T. Optimal Sizing and Techno-Economic Analysis of Grid-Independent Hybrid Energy System for Sustained Rural Electrification in Developing Countries: A Case Study in Bangladesh. *Energies* **2022**, *15*, 6381. [CrossRef]
5. Tarife, R.; Nakanishi, Y.; Chen, Y.; Zhou, Y.; Estoperez, N.; Tahud, A. Optimization of Hybrid Renewable Energy Microgrid for Rural Agricultural Area in Southern Philippines. *Energies* **2022**, *15*, 2251. [CrossRef]
6. Bahramara, S.; Sheikhahmadi, P.; Golpîra, H. Co-optimization of energy and reserve in standalone micro-grid considering uncertainties. *Energy* **2019**, *176*, 792–804. [CrossRef]
7. Ming, M.; Wang, R.; Zha, Y.; Zhang, T. Multi-Objective Optimization of Hybrid Renewable Energy System Using an Enhanced Multi-Objective Evolutionary Algorithm. *Energies* **2017**, *10*, 674. [CrossRef]
8. Kitamura, D.T.; Rocha, K.P.; Oliveira, L.W.; Oliveira, J.G.; Dias, B.H.; Soares, T.A. Planejamento de de Sistemas Híbridos de Energia Elétrica Utilizando Programação Inteira Mista. In Proceedings of the XV Simpósio Brasileiro de Automação Inteligente (SBAI), Rio Grande do Sul, Brazil, 17–20 October 2021; Volume 1. [CrossRef]
9. Tsai, C.T.; Beza, T.M.; Wu, W.B.; Kuo, C.C. Optimal Configuration with Capacity Analysis of a Hybrid Renewable Energy and Storage System for an Island Application. *Energies* **2019**, *13*, 8. [CrossRef]
10. Sawle, Y.; Gupta, S.; Bohre, A.K. Optimal sizing of standalone PV/Wind/Biomass hybrid energy system using GA and PSO optimization technique. *Energy Procedia* **2017**, *117*, 690–698. [CrossRef]
11. Gharibi, M.; Askarzadeh, A. Size and power exchange optimization of a gridconnected diesel generator-photovoltaic-fuel cell hybrid energy system considering reliability, cost and renewability. *Int. J. Hydrogen Energy* **2019**, *44*, 25428–25441. [CrossRef]
12. Nesamalar, J.J.D.; Suruthi, S.; Raja, S.C.; Tamilarasu, K. Techno-economic analysis of both on-grid and off-grid hybrid energy system with sensitivity analysis for an educational institution. *Energy Convers. Manag.* **2021**, *239*, 114188. [CrossRef]
13. López-Salamanca, H.L.; Arruda, L.V.; Magatão, L.; Normey-Rico, J.E. Optimization of Grid-Tied Microgrids Under Binomial Differentiated Tariff and Net Metering Policies: A Brazilian Case Study. *J. Control. Autom. Electr. Syst.* **2018**, *29*, 731–741. [CrossRef]
14. Kitamura, D.T.; Rocha, K.P.; Oliveira, L.W.; Oliveira, J.G.; Dias, B.H.; Soares, T.A. Optimization approach for planning hybrid electrical energy system: A Brazilian case. *Electr. Eng.* **2021**, *1*, 587–601. [CrossRef]
15. Fatih Güven, A.; Mahmoud Samy, M. Performance analysis of autonomous green energy system based on multi and hybrid metaheuristic optimization approaches. *Energy Convers. Manag.* **2022**, *269*, 116058. . [CrossRef]
16. Güven, A.F.; Yörükeren, N.; Samy, M.M. Design optimization of a stand-alone green energy system of university campus based on Jaya-Harmony Search and Ant Colony Optimization algorithms approaches. *Energy* **2022**, *253*, 124089. [CrossRef]
17. Mokhtara, C.; Negrou, B.; Settou, N.; Settou, B.; Samy, M.M. Design optimization of off-grid Hybrid Renewable Energy Systems considering the effects of building energy performance and climate change: Case study of Algeria. *Energy* **2021**, *219*, 119605. [CrossRef]
18. Han, D.; Lee, J.H. Two-stage stochastic programming formulation for optimal design and operation of multi-microgrid system using data-based modeling of renewable energy sources. *Appl. Energy* **2019**, *291*, 116830. [CrossRef]
19. Medina-Santana, A.A.; Cárdenas-Barrón, L.E. Optimal Design of Hybrid Renewable Energy Systems Considering Weather Forecasting Using Recurrent Neural Networks. *Energies* **2022**, *15*, 9045. [CrossRef]
20. Chen, J.; Zhang, W.; Li, J.; Zhang, W.; Liu, Y.; Zhao, B.; Zhang, Y. Optimal Sizing for Grid-Tied Microgrids With Consideration of Joint Optimization of Planning and Operation. *IEEE Trans. Sustain. Energy* **2018**, *19*, 237–248. [CrossRef]
21. Wu, D.; Ma, X.; Huang, S.; Fu, T.; Balducci, P. Stochastic optimal sizing of distributed energy resources for a cost-effective and resilient Microgrid. *Energy* **2020**, *198*, 117284. [CrossRef]

22. Yu, J.; Ryu, J.; Lee, I. A stochastic optimization approach to the design and operation planning of a hybrid renewable energy system. *Appl. Energy* **2019**, *247*, 212–220. [CrossRef]
23. Li, R.; Yang, Y. Multi-objective capacity optimization of a hybrid energy system in two-stage stochastic programming framework. *Energy Rep.* **2021**, *7*, 1837–1846. [CrossRef]
24. Mavromatidis, G.; Orehounig, K.; Carmeliet, J. Design of distributed energy systems under uncertainty: A two-stage stochastic programming approach. *Appl. Energy* **2018**, *222*, 932–950. [CrossRef]
25. Narayan, A.; Ponnambalam, K. Risk-averse stochastic programming approach for microgrid planning under uncertainty. *Renew. Energy* **2017**, *101*, 399–408. [CrossRef]
26. Gazijahani, F.S.; Salehi, J. Optimal Bilevel Model for Stochastic Risk-Based Planning of Microgrids Under Uncertainty. *IEEE Trans. Ind. Inform.* **2018**, *14*, 3054–3064. [CrossRef]
27. Vahedipour-Dahraie, M.; Rashidizadeh-Kermani, H.; Najafi, H.; Anvari-Moghaddam, A.; Guerrero, J.M. Stochastic security and risk-constrained scheduling for an autonomous microgrid with demand response and renewable energy resources. *IET Renew. Power Gener.* **2017**, *11*, 1812–1821. [CrossRef]
28. Sheikhahmadi, P.; Mafakheri, R.; Bahramara, S.; Damavandi, M.Y.; Catalão, J.P.S. Risk-Based Two-Stage Stochastic Optimization Problem of Micro-Grid Operation with Renewables and Incentive-Based Demand Response Programs. *Energies* **2018**, *11*, 610. [CrossRef]
29. Zou, K.; Agalgaonkar, A.P.; Muttaqi, K.M.; Perera, S. Distribution System Planning With Incorporating DG Reactive Capability and System Uncertainties. *IEEE Trans. Sustain. Energy* **2012**, *3*, 112–123. [CrossRef]
30. Liu, Y.; Li, G.; Hou, R.; Wang, C.; Wang, X. A hybrid stochastic/robust-based multi-period investment planning model for island microgrid. *Int. J. Electr. Power Energy Syst.* **2021**, *130*, 106998. [CrossRef]
31. Lai, C.; Jia, Y.; McCulloch, M.; Xu, Z. Daily Clearness Index Profiles Cluster Analysis for Photovoltaic System. *IEEE Trans. Ind. Inform.* **2017**, *13*, 2322–2332. [CrossRef]
32. Nainggolan, R.; Perangin-angin, R.; Simarmata, E.; Tarigan, A.F. Improved the Performance of the K-Means Cluster Using the Sum of Squared Error (SSE) optimized by using the Elbow Method. *J. Phys. Conf. Ser.* **2019**, *1361*, 012015. [CrossRef]
33. Conejo, A.J.; Carrión, M.; Morales, J.M. (Eds.) *Decision Making under Uncertainty in Electricity Markets*; Springer: Berlin/Heidelberg, Germany, 2010. [CrossRef]
34. HOMER. How HOMER Calculates the PV Array Power Output. 2021. Available online: https://www.homerenergy.com/products/pro/docs/latest/how_homer_calculates_the_pv_array_power_output.html (accessed on 23 September 2021).
35. Deotti, L.; Guedes, W.; Dias, B.; Soares, T. Technical and Economic Analysis of Battery Storage for Residential Solar Photovoltaic Systems in the Brazilian Regulatory Context. *Energies* **2020**, *13*, 6517. [CrossRef]
36. GTES *Manual de Engenharia para Sistemas Fotovoltaicos*; CEPEL-CRESEB: Rio de Janeiro, Brazil, 2014.
37. Martinez-Bolanos, J.R.; Udaeta, M.E.M.; Gimenes, A.L.V.; Silva, V.O. Economic feasibility of battery energy storage systems for replacing peak power plants for commercial consumers under energy time of use tariffs. *Energy Storage* **2020**, *29*, 101373. [CrossRef]
38. Cummins. Grupos Geradores. 2021. Available online: https://www.cummins.com.br/ (accessed on 23 September 2021).
39. INMET. Históricos de Dados Meteorológicos. 2021. Available online: https://portal.inmet.gov.br/dadoshistoricos (accessed on 23 September 2021).
40. CEMIG. Valores de Tarifas e Serviços. 2021. Available online: https://www.cemig.com.br/atendimento/valores-de-tarifas-e-servicos/ (accessed on 23 September 2021).
41. MINHA-CASA-SOLAR. 2021. Available online: https://www.minhacasasolar.com.br/ (accessed on 23 September 2021).
42. Nakabayashi, R. *Microgeração Fotovoltaica No Brasil: Viabilidade Econômica*; Technical Report; Instituto de Energia e Ambiente da USP: São Paulo, Brazil, 2015.
43. Solar, C. Canadian Solar CS3W-420P Datasheet. 2023. Available online: https://www.ecorienergiasolar.com.br/assets/uploads/2bcef-canadian_solar-datasheet-hiku_cs3w-p-420_425_430_435_1000v1500v_v5.584.pdf (accessed on 20 January 2023).
44. Solar, C. Canadian Solar CS3W-395P Datasheet. 2023. Available online: https://www.canadiansolar.com/test-au/wp-content/uploads/sites/2/2020/04/Canadian_Solar-Datasheet-HiKu_CS3W-P_v5.59_AU.pdf (accessed on 20 January 2023).
45. Solar, R. Risen Solar RSM156-6-445M Datasheet. 2023. Available online: https://betsolar.es/wp-content/uploads/2020/03/RSM156-6-425-445M-G2.3-Plus-IEC1500V-40mm-2019H2-3-EN.pdf (accessed on 20 January 2023).
46. Solar, C. Canadian Solar CS3W-450MS Datasheet. 2023. Available online: https://www.canadiansolar.com/wp-content/uploads/2019/12/Canadian_Solar-Datasheet-HiKu_CS3W-MS_EN.pdf (accessed on 20 January 2023).
47. ABB. ABB PVS-100/120-TL Datasheet. 2023. Available online: https://loja.l8energy.com/wp-content/uploads/2018/04/Datasheet-PVS-100-120-TL_EN_Rev-G_POR.pdf (accessed on 20 January 2023).
48. Cummins. Cummins C500 D6 Datasheet. 2023. Available online: https://productos.cumminsperu.pe/wp-content/uploads/2018/09/C500D6.pdf (accessed on 20 January 2023).
49. Botelho, D.; de Oliveira, L.; Dias, B.; Soares, T.; Moraes, C. Prosumer integration into the Brazilian energy sector: An overview of innovative business models and regulatory challenges. *Energy Policy* **2022**, *161*, 112735. .: 10.1016/j.enpol.2021.112735. [CrossRef]